

Chapter 4

Evaluation of a PV-driven innovative solar dryer with and without sensible heat storage for *Garcinia pedunculata*: An investigation on kinetics, energy, and economic aspects

Solar dryers are widely used drying units and they are most suitable for drying agricultural products. As discussed in Chapter 3, the utmost significance lies in the dehydration of medicinal fruits like *Garcinia pedunculata* (GP), that are available only during specific seasons, ensuring their accessibility throughout the entire year. The thermal performance, drying kinetics and economic analysis of GP in a Free Convection Corrugated Solar Dryer were explored in the last chapter. Four sets of solar dryer experiments and OSD were considered: an indirect solar dryer without SHS (Exp. I), mixed-mode solar dryer without SHS (Exp. II), an indirect solar dryer with SHS (Exp. III), and mixed-mode solar dryer with SHS (Exp. IV). In literature, both mixed-mode and indirect mode for different products were studied together either replacing only one or two sides of the walls or even in a different set-up [37,102,141,142]. But the facility of the developed dryer for GP is the sliding walls of all the sides of the drying chamber which makes the dryer capable of converting it into any mode as and when necessary. The materials used for the walls of the drying chamber may be changed according to the user's product, usage, need, and economic requirements. As such, the performance study, drying kinetics and economic analysis for drying of GP in an indirect and mixed-mode dryer with and without SHS are reported here. The purpose of the aforementioned comparative study is to evaluate and to compare the parameters for the four configurations.

4.1 Description of forced convection of solar dryer

An experimental set-up for the drying of GP was developed. Photographs of the experimental set-up are shown in Figure 4.1 and Figure 4.2, and the schematic is shown in Figure 4.3. It consisted of a SAC with SHS material (gravels) inside, a drying chamber, a DC fan, five perforated trays, and a Photovoltaic (PV) solar module. The SAC was 1800 mm in length, 800 mm in width, and 150 mm in height. A 4 mm thick glass sheet was used as a cover plate. The corrugated SAC's four sides were composed of 19 cm thick ply boards. The gravels were filled up to the black-colored absorber plate (1600 mm×800 mm×1 cm) within the SAC for SHS. The drying chamber was 0.27 m² in area. The dryer can accommodate maximum 10 perforated trays (0.2 m² each) [143]. The removable chamber

walls are a distinctive characteristic of this developed solar dryer. The same dryer may be run on indirect mode or mixed-mode as and when necessary. The drying chamber in mixed-mode operation absorbs additional solar radiation through the transparent acrylic sheets. The same dryer was also used as an indirect one with its ability to remove the acrylic sheet from the drying chamber. The instruments used and their technical specifications are mentioned in Table 4.1.

Table 4.1 Instruments along with their specifications.

Instrument	Brand	Range	Accuracy
Anemometer	with HTC AVM-06	0-30 ms ⁻¹	± 0.01 ms ⁻¹
RH count Probe		0-80 % RH	± 0.1 % RH
Pyranometer	Amprobe SOLAR-100	0-1999 Wm ⁻²	± 1 Wm ⁻²
Mass balance	A&D Company Limited, HT-120	0-1000 g	± 0.01 g
Data acquisition system with thermocouple (PT:100)	Libratherm	0 to 200 °C	± 0.1 °C
Photovoltaic Module	Solar Loom Solar	Peak power output: 125 W, Operating voltage: 12V, Panel Technology: Mono Perc	
DC fan	Rashri	12 V DC, maximum current 1 A, 2000 rpm	



Figure 4.1 Active indirect solar dryer with corrugated SAC.



Figure 4.2 Active mixed-mode solar dryer with corrugated SAC.

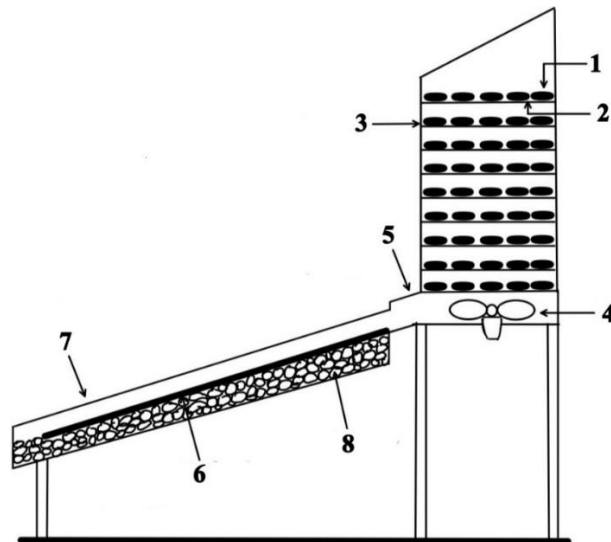


Figure 4.3 Schematic of solar dryer integrated with corrugated SAC.

1) Medicinal fruit (GP), 2) Perforated trays, 3) Interchangeable walls of drying chamber, 4) DC Fan, 5) Connecting channel, 6) Corrugated absorber plate, 7) Glass plate, 8) Gravels, 9) Laptop, 10) Data acquisition system, 11) Thermocouple, 12) Photovoltaic Solar Module, 13) Pyranometer, 14) Thermocouple, 15) Anemometer with RH count Probe

4.2 Working principle of the dryer

The primary source of energy for this drying system was solar energy with the use of SAC. The SAC is made of a transparent cover and an absorber plate. It is integrated with the drying chamber and has an angle of 26° towards the south to achieve maximum radiation. The corrugated absorber plate was painted black for maximum absorption of solar energy. For SHS, the gravels were filled inside the SAC up to the black-coloured absorber plate. The stand of the collector was made adjustable to use in all seasons. The sensible heat storage materials stored heat during the daytime and released it when there was not sufficient radiation from the sun for drying the GP. A fraction of the incident ray was reflected in the ambient, and another fraction was transmitted through the cover. The black-painted corrugated plate of the solar collector absorbed a part of the solar energy. A substantial portion of the heat absorbed by the corrugated plate was convected to heat the air inside the chamber. The air leaving the SAC entered the dryer via a DC fan located at the entry of the dryer. The fan sucked the outgoing hot air from the SAC and created a forced draft inside the dryer. This hot air circulates steadily and continuously over GP and removes the moisture from it. Sliced GP are kept in five perforated trays inside the chamber. The temperature of the product increases inside the chamber, and the MC reduces subsequently. A Photovoltaic solar module was used to run the DC fan. The installation of this solar dryer in rural areas with sensible heat storage is trouble-free as the materials are readily available, and the design is not very complicated. In mixed-mode operation, the drying chamber absorbs additional solar radiation through the transparent acrylic sheets.

4.3 Experimental procedure

The experiments in the active solar dryer were done in April and May 2021. For the evaluation of corrugated solar air heating system, standard dimensions were used [144]. These experiments were carried out between 9:00 h to 16:00 h in the solar dryer without SHS and 9:00 h to 18:00 h in the solar dryer with SHS on different days. 5 kg of fresh GP were bought from the local market, washed with water, and sliced. The experiments were carried out in five trays. Prior to the experiment, the dryer was preheated for 1 h. The GP-loaded trays were then placed inside the solar dryer. The fan at the bottom of the dryer was run by the Photovoltaic solar module. The solar radiation, ambient temperature, ambient relative humidity, inlet, and outlet temperatures of SAC and dryer, relative humidity of air in the dryer, and weight loss were recorded at every 1 h interval. The relative humidity was

measured at multiple locations at each cross section of the dryer and the average values were reported.

Figure 4.4 gives the complete method followed during the experiments. A sample tray of 250 g was kept inside the dryer for all the experiments to study the drying kinetics of GP. Another 5 kg of GP was placed for OSD. The hot air oven method was used to note the initial MC. The thermal efficiency of SAC, the efficiency of the dryer, SEC, MR, MC, and the drying rate for all the experiments were calculated with the help of the experimental data. To determine the possible errors, 12 systematic drying runs comprising three replicates were done for each mode of the dryer. A well-replicated experiment assures that the relationship between the independent and dependent variables is genuine and reliable.

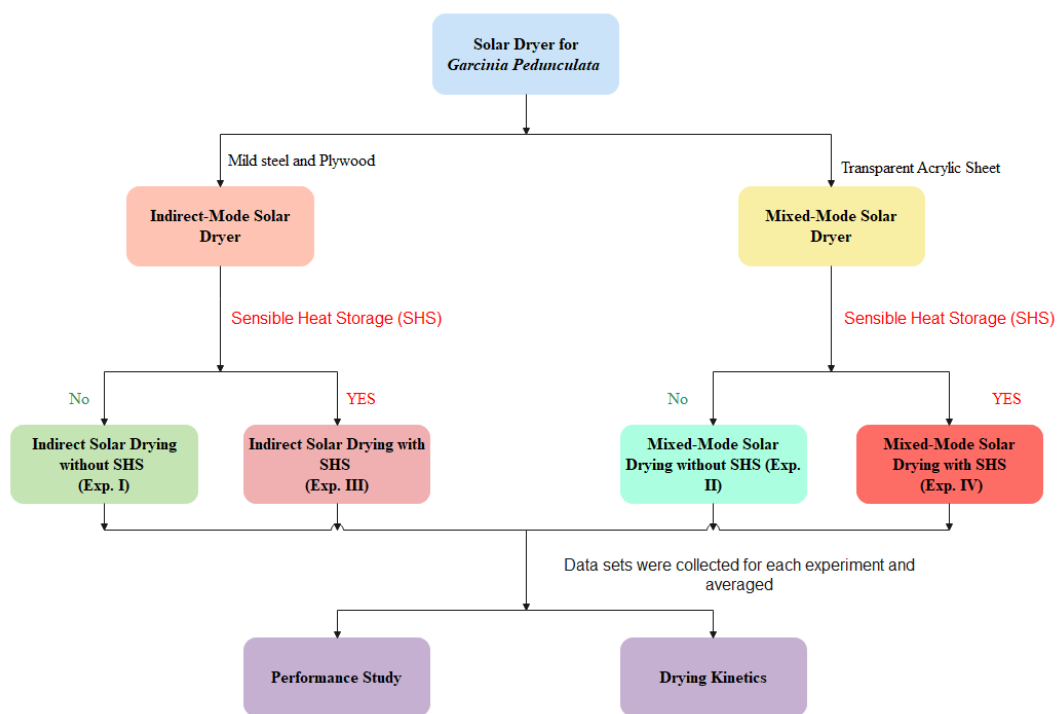


Figure 4.4 Diagram representation of the methodology followed for drying of *Garcinia pedunculata*.

4.4 Results and Discussion

The weather conditions were all reported for similar sunny days. The experiments for the indirect solar dryer without SHS (Exp. I) were performed on Day 1 and continued till Day 2. The mixed-mode solar dryer with SHS (Exp. II) was performed on Day 3 and continued till Day 4. In addition, open sun-drying OSD was also carried from Day 1 to Day 3. An indirect solar dryer with SHS (Exp. III) was performed on Day 5 and continued till

Day 6, and on Day 7, the experiment for a mixed-mode solar dryer with SHS (Exp. IV) was performed.

Table 4.2 Values of uncertainties of the different parameters in the experiment.

Parameter	Average Uncertainty
Moisture loss (weight)	± 0.01 (g)
Temperature	± 0.1 ($^{\circ}\text{C}$)
Air velocity	± 0.01 (ms^{-1})
Solar radiation	± 1 (Wm^{-2})
Thermal efficiency in SAC	± 2.09 (%)
Thermal efficiency of the dryer	± 2.75 (%)

4.4.1 Performance study of drying *Garcinia pedunculata*

The experiments for Exp. I and Exp. II were performed from 9:00 h to 16:00 h and from 9:00 h to 18:00 h for Exp. III and Exp. IV. All four modes in the solar dryer were performed for forced convection. To avoid the reabsorption of moisture, the dried products were kept in airtight containers.

Experiments without SHS

The climatic conditions during solar drying of GP are shown in Figure 4.5. The average ambient temperatures for Day 1 and Day 2 varied in the range of 29.3 $^{\circ}\text{C}$ to 34.1 $^{\circ}\text{C}$ and 30.2 $^{\circ}\text{C}$ to 35.4 $^{\circ}\text{C}$, respectively. The corresponding ranges for Day 3 and Day 4 were 29.8 $^{\circ}\text{C}$ to 34.7 $^{\circ}\text{C}$ and 29.1 $^{\circ}\text{C}$ to 34.1 $^{\circ}\text{C}$. The solar radiation reached its peak at 11:00 h on each day and subsequently decreased in the afternoon on all four days. The maximum solar radiation on Day 1, Day 2, Day 3, and Day 4 were 902, 920, 918, and 908 W/m^2 , respectively.

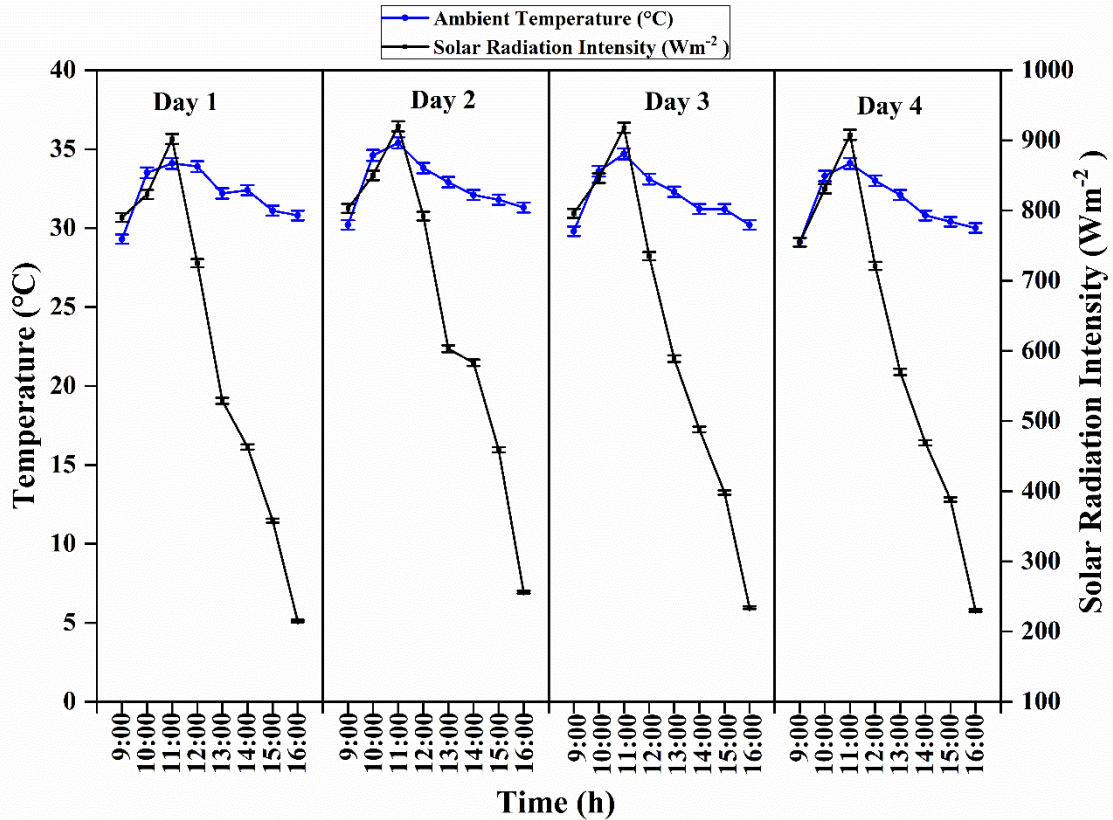


Figure 4.5 Variations of Solar radiation and ambient temperature with time during Exp. I and Exp. II.

The variations of SAC inlet temperature, SAC outlet temperature, dryer inlet temperature, and dryer outlet temperature with time for Exp. I and Exp. II are plotted in Figure 4.6. The average inlet temperatures of SAC on Day 1, Day 2, Day 3, and Day 4 were observed as 34.6 °C, 35.1 °C, 34.9 °C, and 34.2 °C, respectively. The air mass flow rate was 0.02 kg/s. Furthermore, the average outlet temperatures of SAC were 57.3 °C, 59.7 °C, 58.5 °C, and 56.9 °C, respectively on Day 1, Day 2, Day 3, and Day 4. The solar drying of GP in Exp. I took 31 h or 2 days. The inlet temperature of the dryer varied between 38.9 °C-66.4 °C for Exp. I and 39.2 °C-71.3 °C for Exp. II. The outlet temperature of the dryer varied in the range of 37.5 °C to 58.4 °C for Exp. I and 38.1 °C and 64.5 °C for Exp. II. The time required for drying was 26 h for Exp. II. As expected, the maximum temperature was observed at 11:00 am. Temperatures decreased as the intensity of radiation from the sun decreased subsequently. Additionally, the dryer inlet temperature of mixed-mode (Exp. II) was 4.9 °C more than the indirect mode (Exp. I) at 11:00 am. Moreover, it took around 5 h less in Exp. II than in Exp. I to complete the drying process. This is due to the drying chamber being covered with plywood in indirect mode, that prevented solar radiation from

penetrating the food. The OSD of GP required around 53 h to reach the final MC of 12.09 % (w.b.). The relative humidity of the ambient and dryer for Exp. I and Exp. II is plotted in Figure 4.7. The variations in the relative humidity of the dryer for Exp. I and Exp. II reached its lowest at 17.8 % and 12.7 %, respectively.

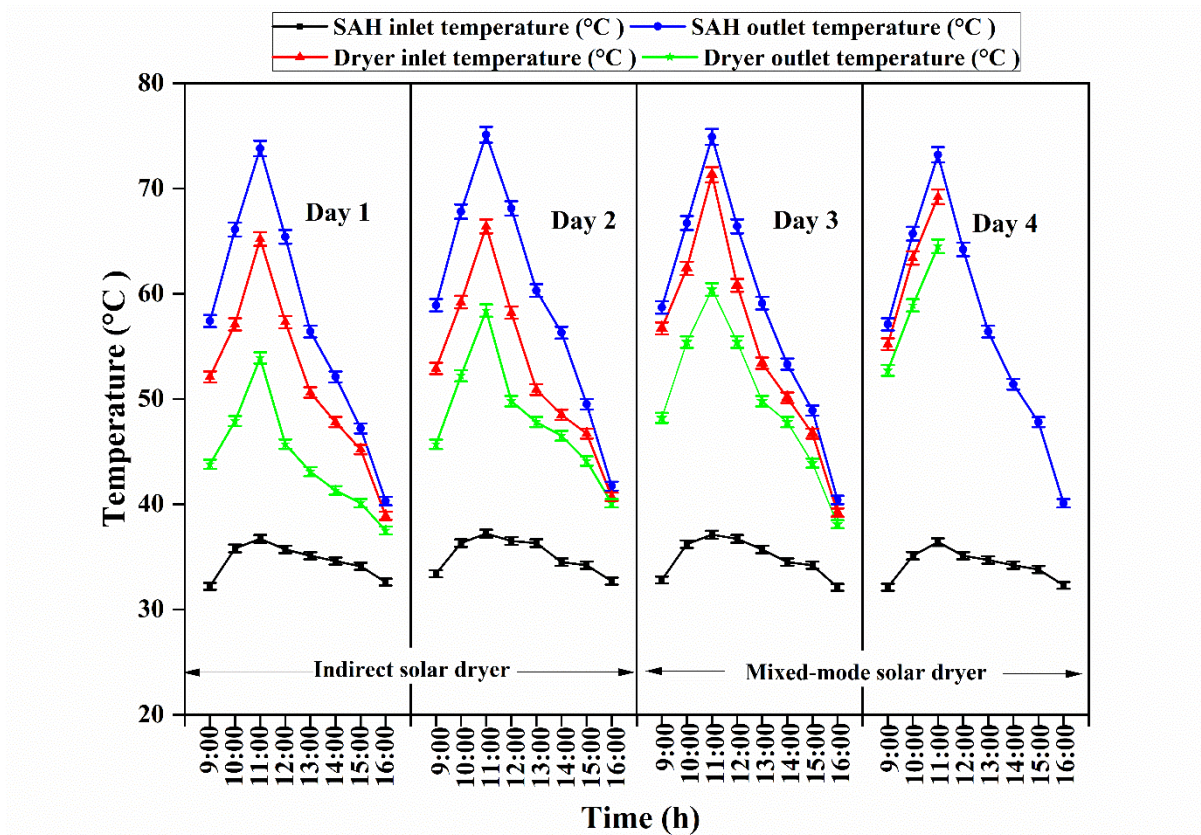


Figure 4.6 Variations of SAC inlet temperature, SAC outlet temperature, dryer inlet temperature, dryer outlet temperature with time for Exp. I and Exp. II.

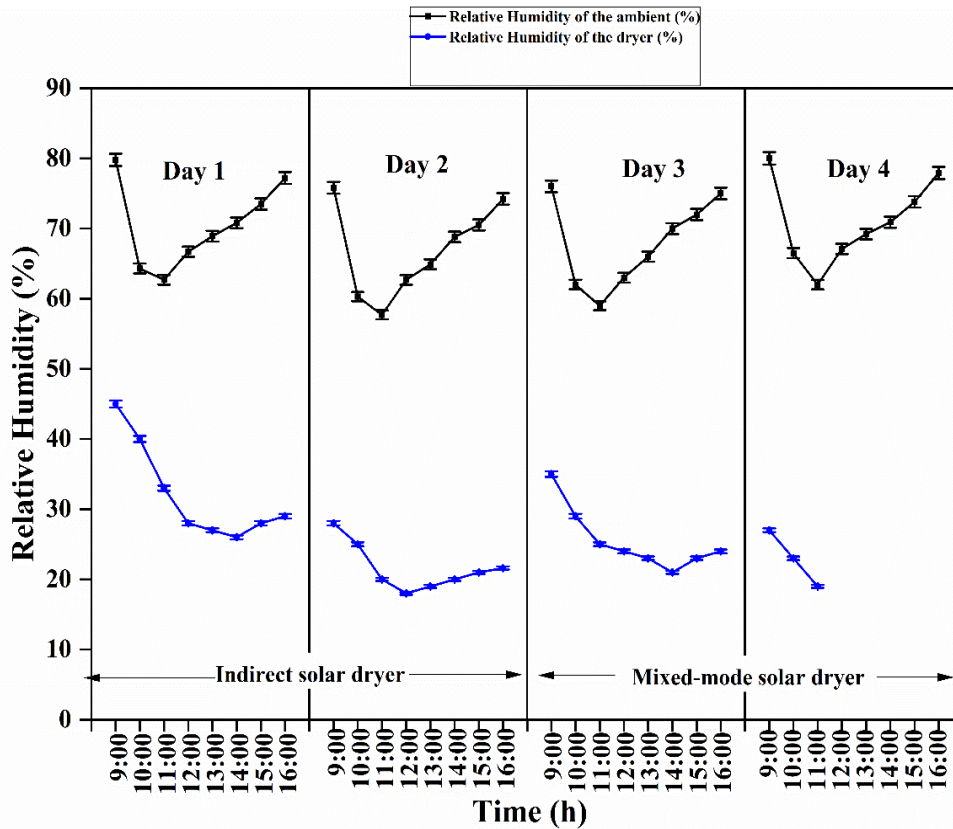


Figure 4.7 Variations of relative humidity of the ambient and relative humidity of dryer with time for Exp. I and Exp. II.

The variations in the thermal efficiency of SAC on Day 1, Day 2, Day 3, and Day 4 are shown in Figure 4.8. The SAC efficiency as per Eq. (3.9) depends upon the mass-flow rate, inlet, and outlet temperatures, SAC area, and solar radiation incident on it. These efficiencies were estimated without the energy storage material. The absorber plate (black coated) was a corrugated aluminium plate. The reasons to use the corrugated SAC in place of others are higher outlet temperature, increased heat transfer, and hence higher thermal efficiency [145]. The average efficiencies were 66.71 %, 65.45 %, 66.56 %, and 65.44 %, respectively, on Day 1, Day 2, Day 3, and Day 4. All the efficiencies were maximum at 11:00 h.

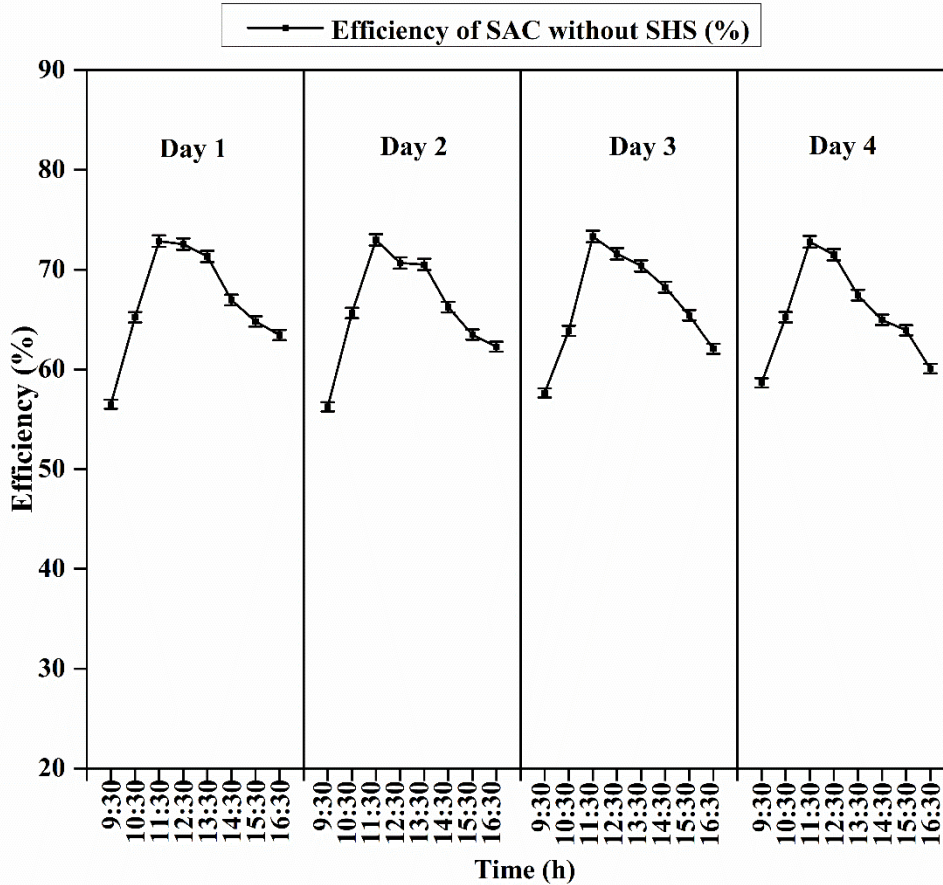


Figure 4.8 Variations of energy efficiency of SAC without SHS with time

The variations of SEC and efficiency for Exp. I and Exp. II were calculated by Eqs. (3.11) and (3.12), respectively, and plotted in Figure 4.9. The Exp. I was done on Day 1, and it continued till Day 2. On Day 2, as the MC of the material being dried decreased, the energy utilization to evaporate the remaining moisture also decreases. This means that the dryer needs to utilize less heat energy near completion of drying which results in a decrease in thermal efficiency. The maximum efficiency was calculated as 40.11 % with an average of 18.12 %. Exp. II was performed on Day 3 and continued till Day 4. Exp. II was performed on Day 3 and continued till Day 4. It is observed that the efficiency on the Day 4 is significantly less than the corresponding values during Exp. II. This is due to the higher moisture removal rate in the mixed-mode on the first day of the Exp. II (Day 3) and lower moisture removal rate on the second day (Day 4) due to the near completion of the drying process. It exhibited the maximum efficiency (41.15 %) at 11:00 h with an average of 22.37 %. This leads to the shorter time required for drying GP. The lowest SEC for Exp. I and Exp. II were calculated as 5.87 and 5.73 kWh/kg, respectively. A comparative analysis of the present dryer with different dryers without storage available in the literature is shown in

Table 4.3. It is clear from Table 4.3 that the present solar dryer's average thermal efficiency is comparable to or better than the other previously studied similar solar dryers.

Table 4.3 Comparative analysis of present dryer with different dryers without storage.

Sl. No.	Experiments	Type of dryers	Drying time (h)	Efficiency (%)	Product used for Drying
1	Present Study (Exp. I)	Indirect	31	18.12	GP
2	Present Study (Exp. II)	Mixed-mode	26	22.37	GP
3	Fudholi <i>et al.</i> [146]	Indirect	33	13	Red chili
4	César <i>et al.</i> [34]	Indirect	26	8.80	Tomato
		Mixed-mode	17	10.66	Tomato

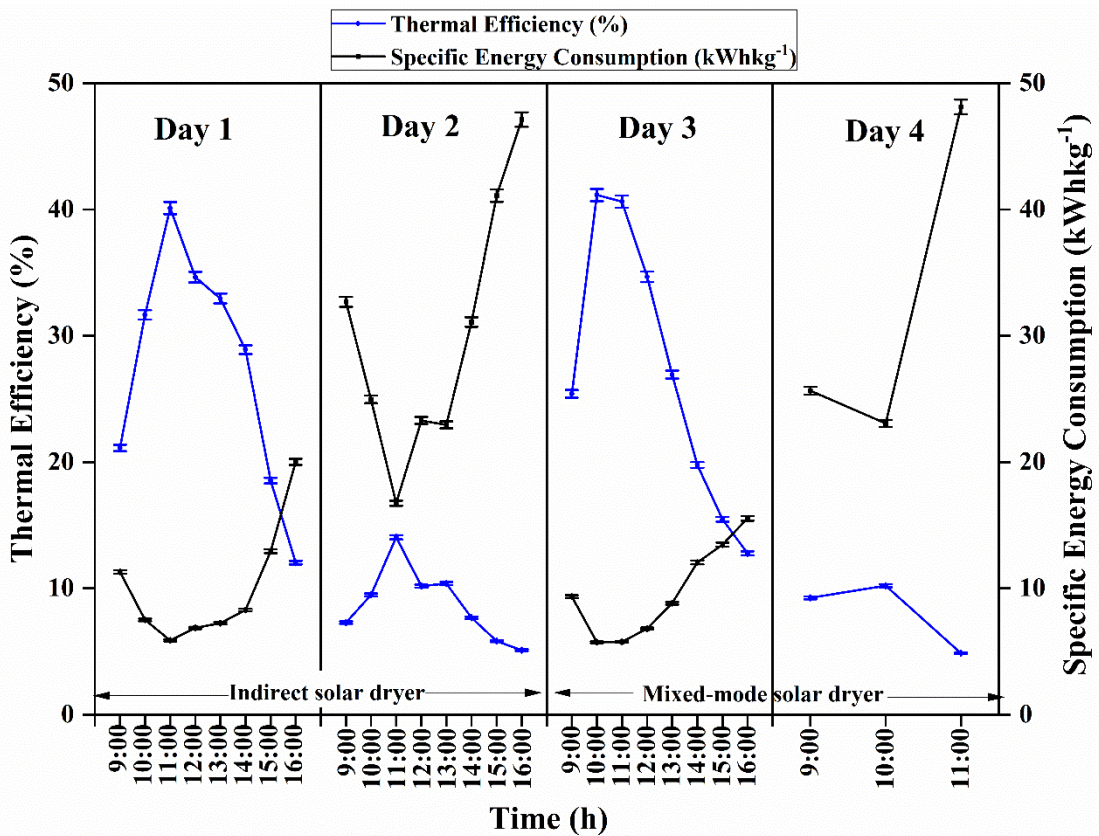


Figure 4.9 Variations of thermal efficiency and SEC of the dryer with time for Exp. I and Exp. II.

Experiments with SHS

The ambient conditions for Exp. III and Exp. IV are presented in Figure 4.10. The experiments were carried out with SHS material from 9:00 h to 18:00 h. Seventy kg of gravels (density=1840 kg/m³, thermal conductivity=0.3-0.5 W/mK) [147] were used as the SHS material that was placed below the corrugated absorber plate. The maximum solar radiation intensity on Day 5, Day 6, and Day 7 were 914, 923, and 936 W/m² at 11:00 h. The ambient temperatures varied in the range of 29.8 °C to 36.1 °C on Day 5, 30.1 °C to 35.2 °C on Day 6, and 30.8 °C to 36.1 °C on Day 7.

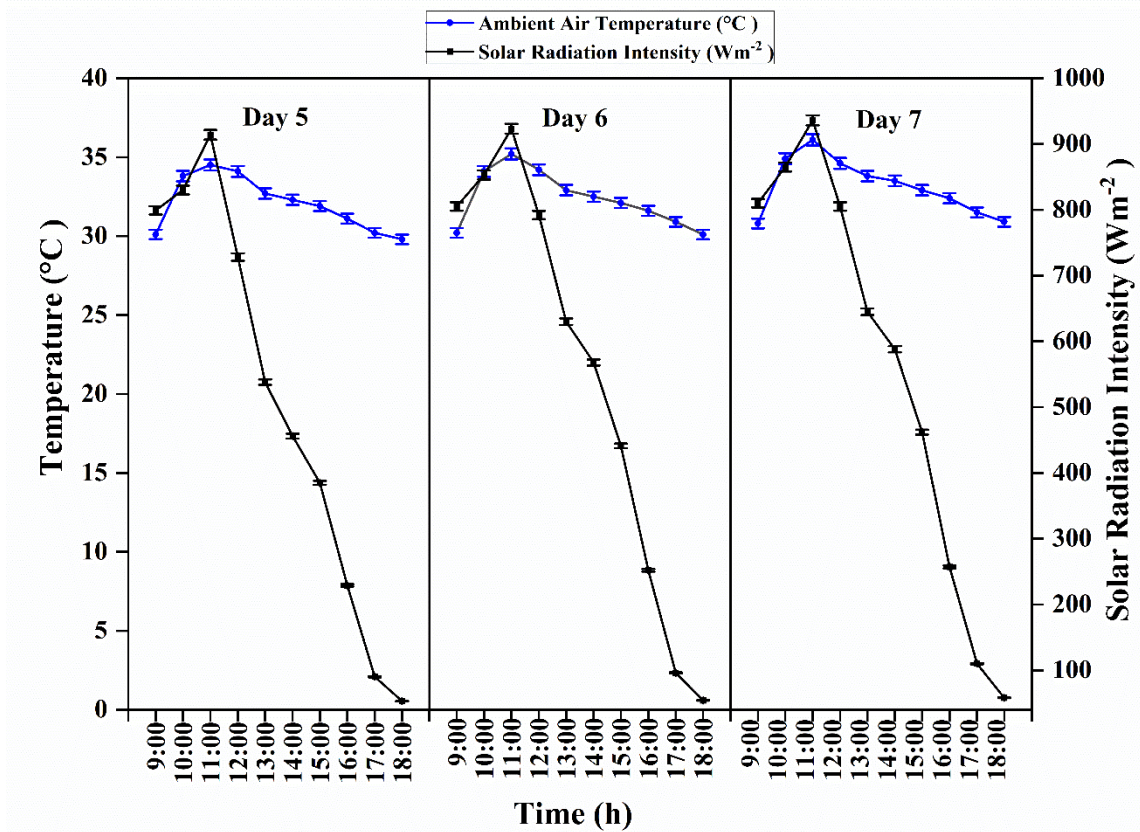


Figure 4.10 Variations of solar radiation and ambient temperature with time during Exp. III and Exp. IV.

The variations of SAC inlet temperature, SAC outlet temperature, dryer inlet temperature, and dryer outlet temperature with time for Exp. III and Exp. IV are plotted in Figure 4.11. It was observed that during the initial hour, SAC outlet temperature with SHS material was somewhat lesser than the corresponding temperature without SHS for similar solar radiation intensity. However, during the latter half of the day, the outlet temperature increased in the SAC with SHS material than the one without SHS because of the heat

absorbed by the SHS material. It was also witnessed that the temperature of the outlet of SAC with SHS was (2.5-6.7) °C more than the ambient temperature during 17:00-18:00 h. This is because the heat is stored in these SHS materials during the daytime and released when there is not sufficient radiation from the sun. The average inlet temperature of SAC was 35.3 °C, 35.4 °C, and 35.9 °C, respectively on Day 5, Day 6, and Day 7. In addition to this, the range of outlet temperatures of the SAC was 36.3-73.6 °C, 36.7-73.9 °C, and 37.6-75.1 °C, respectively, on Day 5, Day 6, and Day 7. The dryer inlet temperature varied in the range of 35.5-67.9 °C for Exp. III and 36.1-71.9 °C for Exp. IV. The drying time for these Exp. III (indirect with SHS) was 28 h. However, the drying time for Exp. IV (mixed mode with SHS) was 10 h. The dryer outlet temperature varied in the range of 34.8-61.2 °C for Exp. III and 35.2-60.5 °C for Exp. IV. The variations of relative humidity of the ambient and dryer are plotted in Figure 4.12. The lowest relative humidity of the dryer was recorded at 17.2 % and 10.1 % for Exp. III and Exp. IV, respectively.

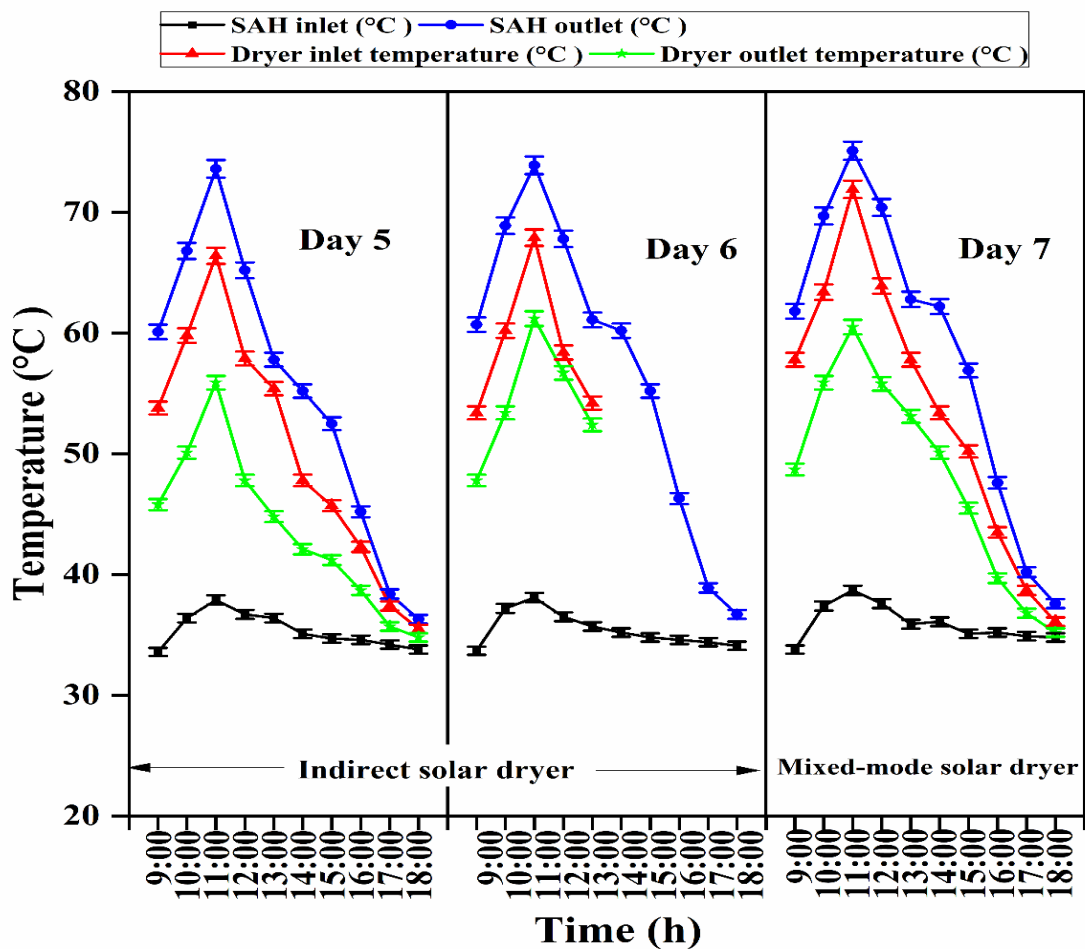


Figure 4.11 Variations of SAC inlet temperature, SAC outlet temperature, dryer inlet temperature, dryer outlet temperature with time for Exp. III and Exp. IV.

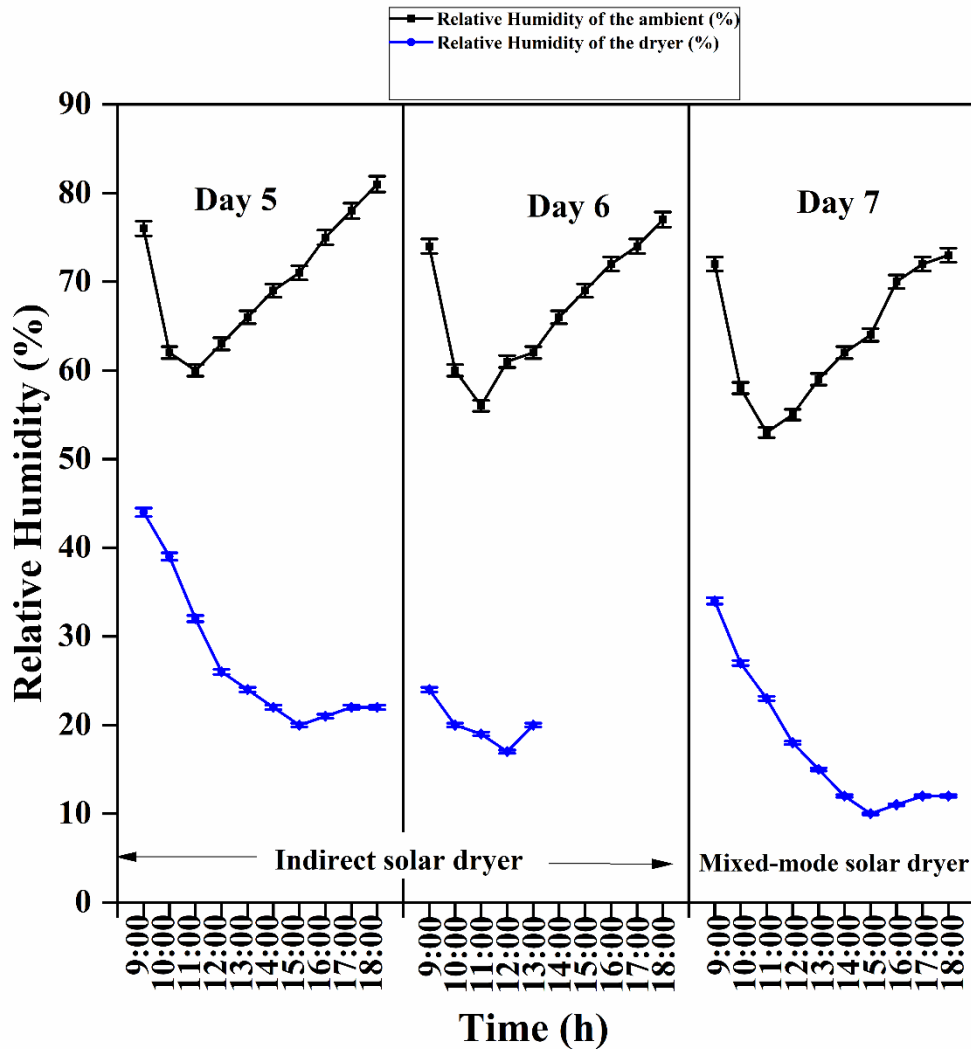


Figure 4.12 Variations of relative humidity of the ambient and relative humidity of dryer with time for Exp. III and Exp. IV.

When design, material, availability, and cost are counted upon, solar dryers with SHSs are much simpler. The medium for SHS can be of two types: solids (pebbles, gravels, brick, concrete, etc.) and liquids (water, molten salts, petroleum oils, etc.). The stored energy in SHS is charged and discharged in due course of time [100,148]. The variation of thermal efficiency of SAC with SHS, calculated with Eq. (3.9), is shown in Figure 4.13. The average energy efficiencies of SAC with SHS were 74.08 %, 74.60 %, and 76.09 %, respectively. The value of the SAC with SHS was consistently found to be higher than the SAC without SHS when comparing the outlet air temperatures of the SACs. As a result, it was observed that the SAC without SHS was less efficient than SAC with SHS at the same mass flow rate. During the former half of the day, the efficiencies of both the cases (without and with SHS) were similar but after 12:30 h the efficiency of the SAC without storage decreased whereas the one with storage increased. The efficiency of SAC with SHS has sharply increased as a

result of energy storage, which captured excess energy in the morning and discharged it in the evening.

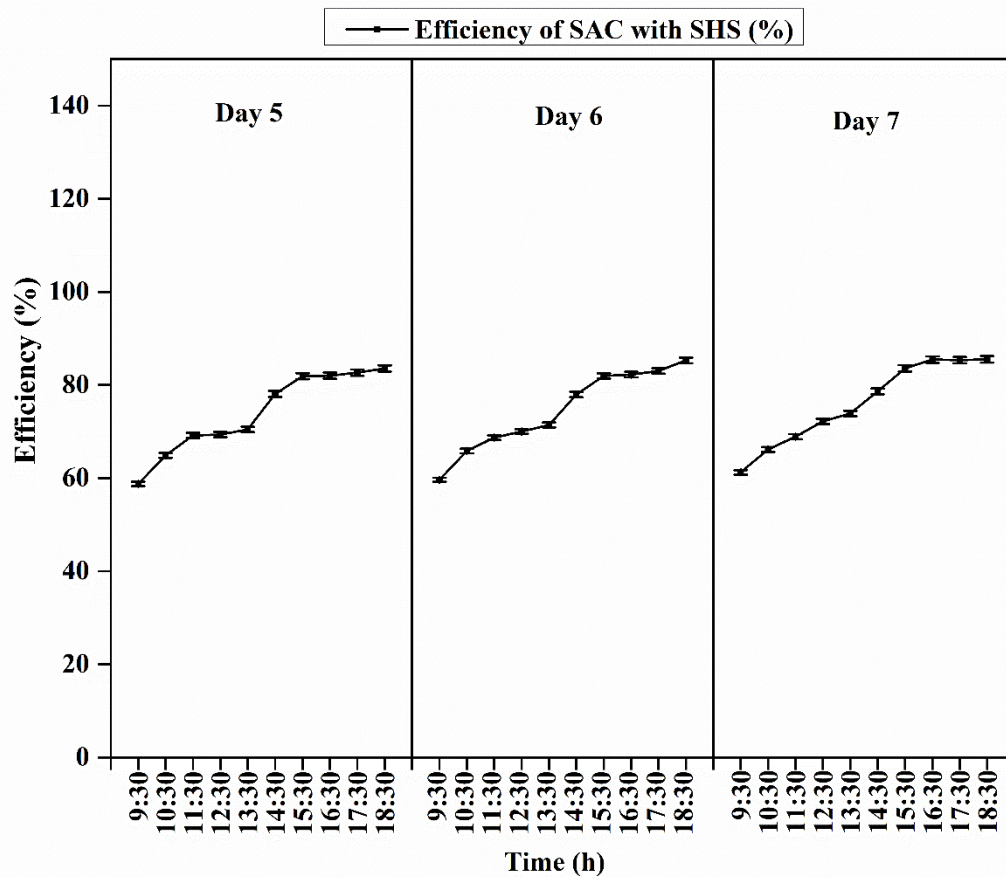


Figure 4.13 Variations of energy efficiency of SAC with SHS with time

The SEC and thermal efficiency for Exp. III and Exp. IV calculated using Eqs. (3.11) and (3.12) are plotted in Figure 4.14. The maximum efficiencies for Exp. III and Exp. IV were calculated as 40.51 % and 44.25 %, respectively. Exp. III and Exp. IV had average efficiencies of 21.74 % and 24.46 %, respectively, and took 28 h and 10 h to dry, respectively. In comparison to similar studies, [84] developed a mathematical model to explain an active solar collector with SHS material (pebble) for drying of bitter melon. The drying time was 7 h with a drying efficiency of 19 %. In another study, [47] compared different SHS materials, including concrete, sand, and rock bed, to investigate their thermal performance. The drying times for Copra in a greenhouse dryer using concrete, sand, and rock bed were 78 h, 66 h, and 53 h, respectively, with dryer efficiencies of 9.5 %, 11 %, and 11.65 %, respectively. The developed dryer in the present study showed improved results. The summary is given in Table 4.4. Comparing Exp. I and Exp. III, the incorporation of SHS material increased the average efficiency from 18.12 % to 21.74 %. Similarly, the average

efficiency increased to 24.46 % in Exp. IV from 22.37 % in Exp. II. The lowest SEC for Exp. III and Exp. IV were 5.81 and 5.33 kWh/kg, respectively. Considering all four experiments in the solar dryer, Exp. I had the minimum and Exp. IV had the maximum efficiency. Along with the high moisture removal rate in the mixed-mode solar dryer, the SHS material inside the SAC in Exp. IV led to higher efficiency and lower SEC.

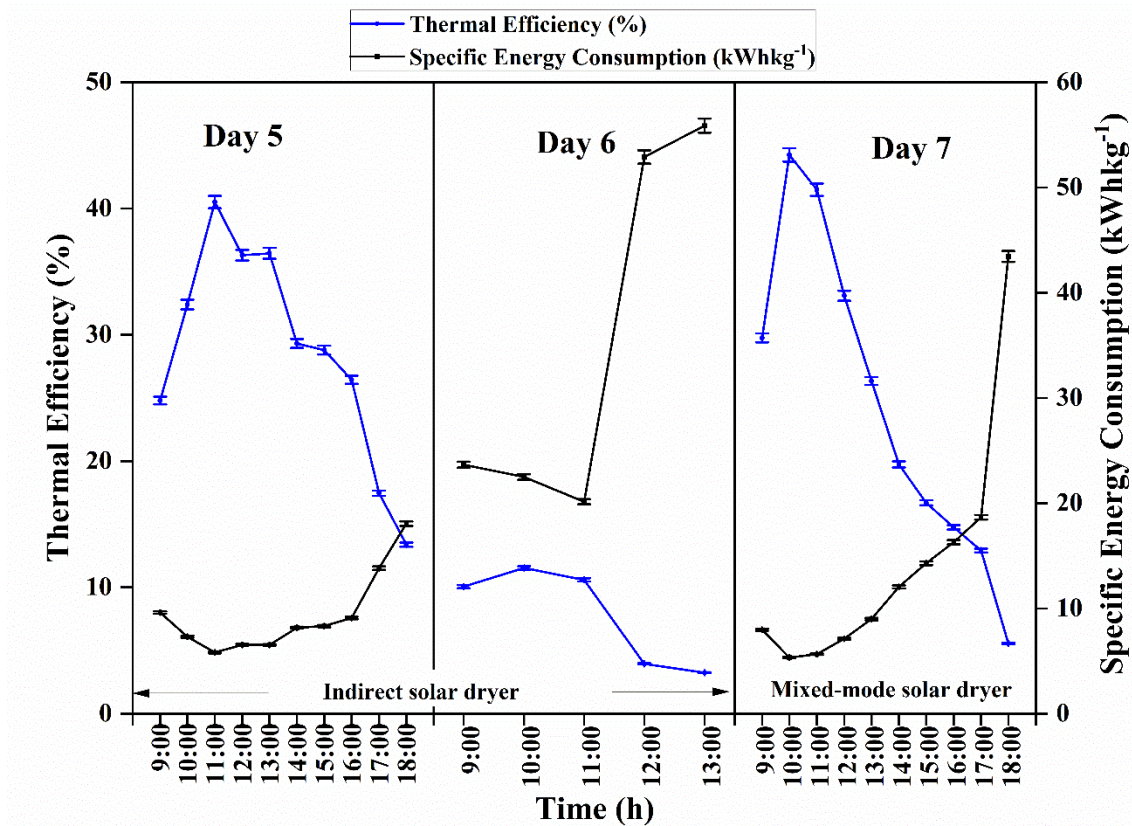


Figure 4.14 Variation of thermal efficiency and SEC of the dryer with time for Exp. III and Exp. IV.

Table 4.4 Comparative analysis of present dryer with different dryers with storage.

Sl. No	Experiments	Type of dryer	Type of TES	Drying time (h)	Efficiency (%)	Product used for Drying
1	Present Study (Exp. III)	Indirect	Gravels	28	21.74	GP
2	Present Study (Exp. IV)	Mixed mode	Gravels	10	24.46	GP
3	Vijayan <i>et al.</i> [84]	Indirect	Pebble	7	19	Bitter Gourd
4	Ayyappan <i>et al.</i> [47]	Greenhouse	Concrete sand rock-bed	78 66 53	9.5 11 11.65	Copra

4.4.2 Drying kinetics

This section presents the drying kinetics of *Garcinia pedunculata* for different experiments from an initial MC of 87.99 % (w.b.) to a final MC of 12.09 % (w.b.). The total drying times were 31, 26, 53, 28, and 10 h for Exp. I, Exp. II, OSD, Exp. III and Exp. IV, respectively. It can be noted that the drying time was the least in Exp. IV and most in OSD. The temperature inside the mixed-mode was sufficiently higher than the indirect-mode. This is because of the experiments in Exp. II and Exp. IV added supplementary solar radiation using the cabinet's transparent cover. Additionally, SHS material inside the SAC increased the inlet temperature of the dryer during the low radiation period. The variation of MR and drying rate with drying time are discussed here. Eleven models available in the literature were evaluated for the selection of suitable drying models for the four sets of experiments in the solar dryer and OSD. Figure 4.15 gives the drying rate versus time graph for Exp. I, Exp. II and OSD. The drying rate in OSD was observed slower than Exp. I and Exp. II. Figure 4.16 shows the variation of drying rate with drying time for Exp. III and Exp. IV. Comparing all the experiments, the drying rate was fastest in Exp. IV and least in OSD. Moreover, the maximum drying rate was observed at 11:00 h that was during the peak solar radiation hour for all experiments. At the latter part of the day, the drying rate decreased for all the experiments due to the slower removal of moisture from GP slices.

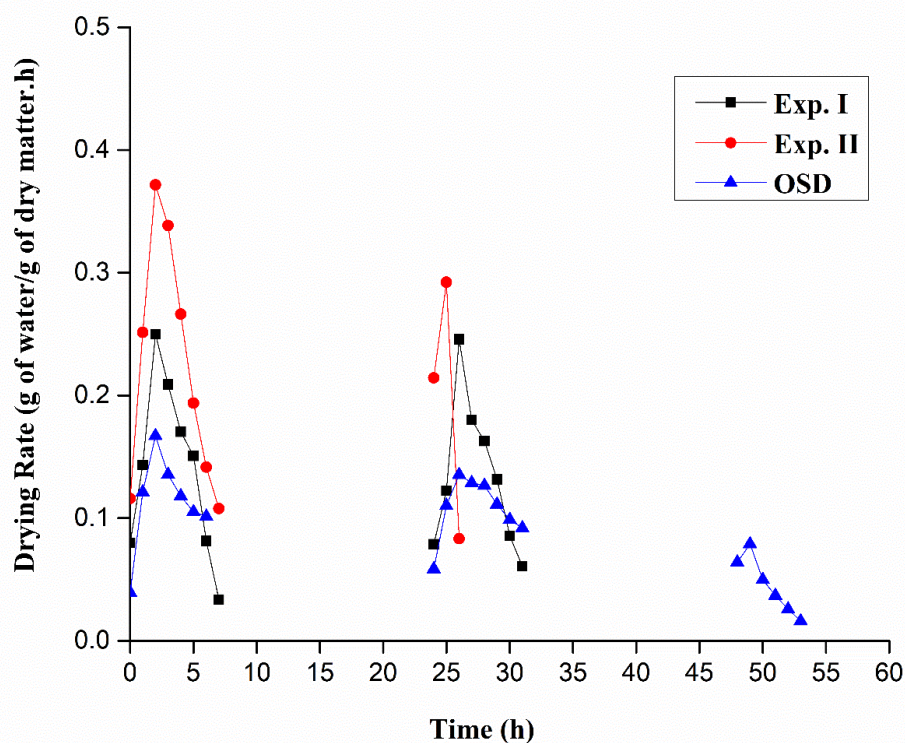


Figure 4.15 Variation of drying rate with drying time for Exp. I, Exp. II and OSD.

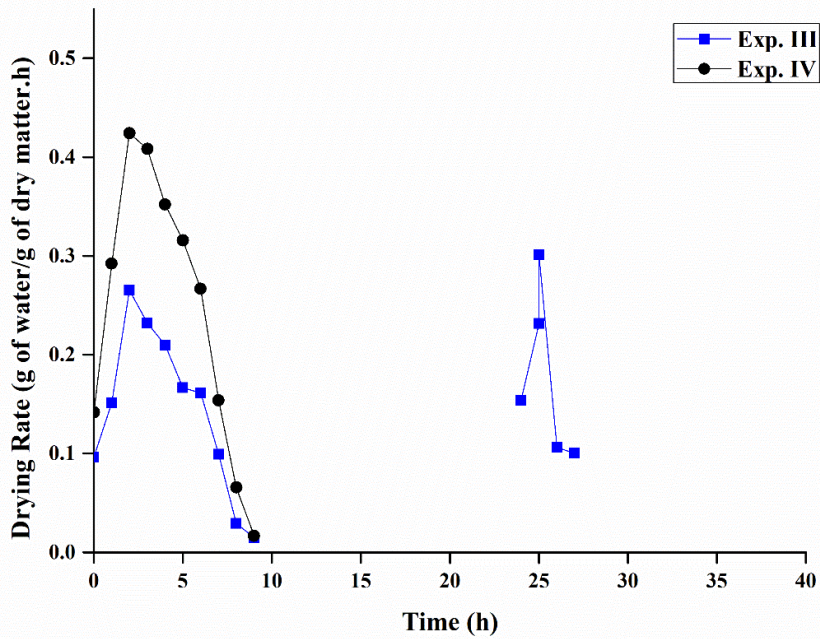


Figure 4.16 Variation of drying rate with drying time for Exp. III and Exp. IV.

Figure 4.17 exhibits the variation of MR as a function of drying time for Exp. I, Exp. II and OSD. The non-linear regression evaluation of MR versus drying time is necessary to find the best-fitted drying model from the eleven models in Table 3.2. Figure 4.18 gives the MR versus drying time for Exp. III and Exp. IV. Table 4.5, Table 4.6, and Table 4.7 summarize the regression analysis for Exp. I, Exp. II and OSD, respectively. Similarly, Table 4.8 and Table 4.9 gives the regression analysis for Exp. III and Exp. IV, respectively. All the eleven models were evaluated to check the best-suited model following the highest value of R^2 and lowest values of χ^2 , and $RMSE$. Fulfilling the mentioned conditions, the best-fit model was Two-Term for Exp. I, Exp. II, OSD and Exp. III. Midilli and Kucuk model was observed to be the best-fitted model for Exp. IV. The values were $R^2 = 0.9929$, $\chi^2 = 0.0005139$, and $RMSE = 0.02449$ for Exp. I; $R^2 = 0.9973$, $\chi^2 = 0.00024$, and $RMSE = 0.01764$ for Exp. II; $R^2 = 0.9889$, $\chi^2 = 0.00347$, and $RMSE = 0.03198$ for OSD; $R^2 = 0.9912$, $\chi^2 = 0.00066$, and $RMSE = 0.02795$, for Exp. III and $R^2 = 0.9998$, $\chi^2 = 0.000020$, and $RMSE = 0.005261$ for Exp. IV.

The Two-Term model for Exp. I is given as:

$$MR = 0.7949 \exp(-0.114 t) + 0.4999 \exp(-1.092 t) \quad (4.1)$$

The Two-Term model for Exp. II is given as:

$$MR = 0.6604 \exp(-0.715 t) + 0.5498 \exp(-0.1395 t) \quad (4.2)$$

The Two-Term model for OSD is given as:

$$MR = 0.0001 \exp(0.3112 t) + 1.036 \exp(-0.1351 t) \quad (4.3)$$

The Two-Term model for Exp. III is given as:

$$MR = 0.5392 \exp(-0.09363 t) + 0.4829 \exp(-0.3671 t) \quad (4.4)$$

The Midilli and Kucuk model for Exp. IV is given as:

$$MR = 1.002 \exp(-0.2851 t^{1.185}) + 0.01305 t \quad (4.5)$$

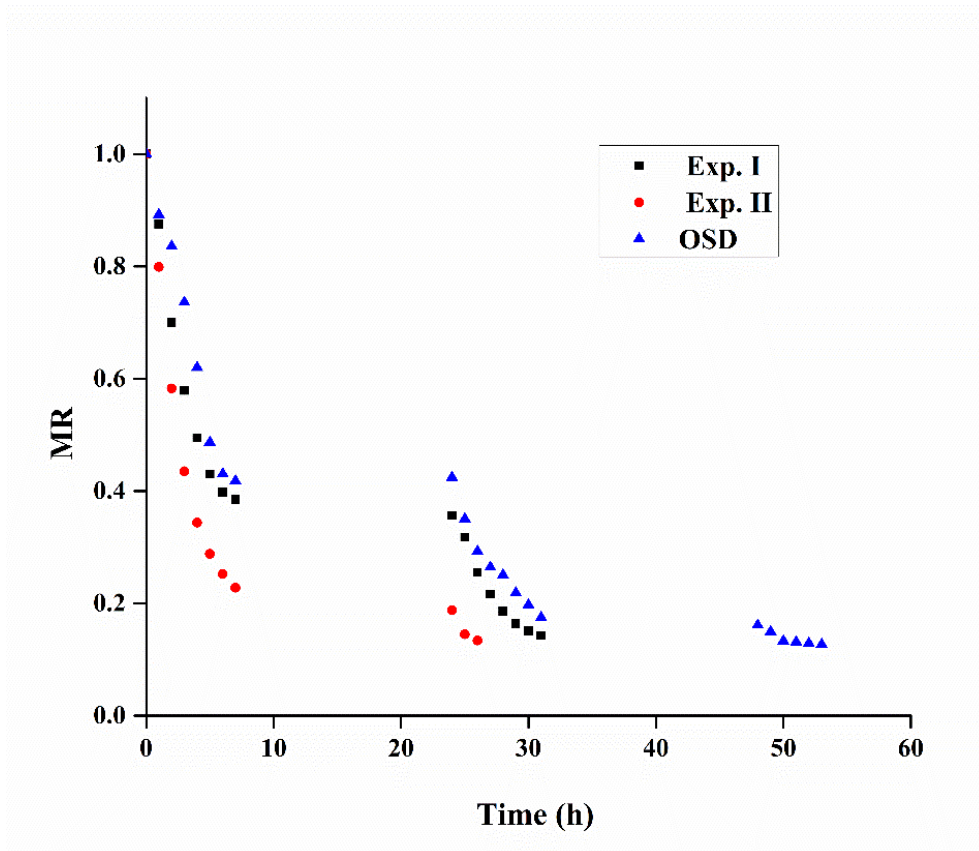


Figure 4.17 Variation of MR with drying time for Exp. I, Exp. II and OSD.

Figure 4.19, Figure 4.20 and Figure 4.21 show the comparison of experimental and predicted MR for Exp. I, Exp. II and OSD using the Two-Term model. In the same way, Figure 4.22 and Figure 4.23 show the comparison of experimental and predicted MR for Exp. III and Exp. IV using the Two-Term model and Midilli and Kucuk model, respectively. The straight line for Exp. I and Exp. II validates the model's suitability, as can be seen in these figures.

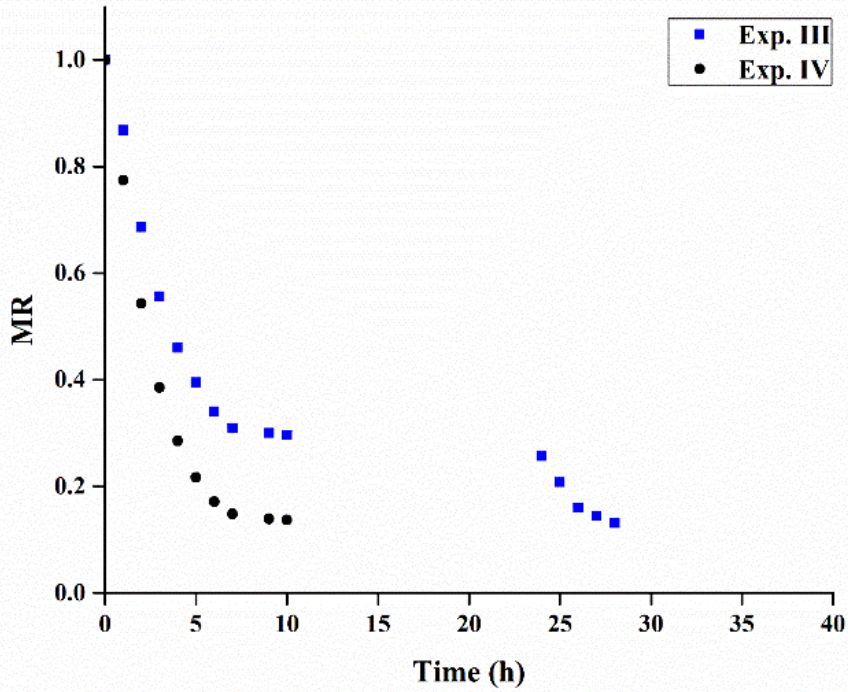


Figure 4.18 Variation of MR with drying time for Exp. III and Exp. IV.

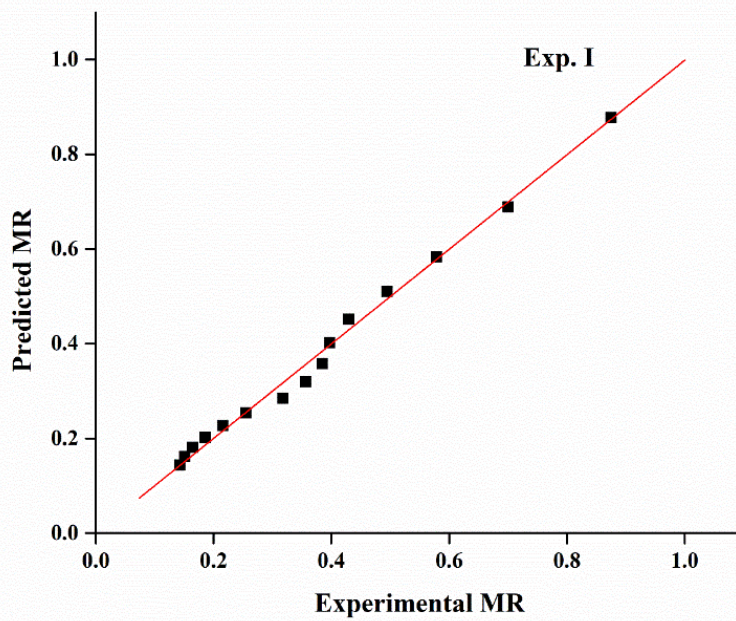


Figure 4.19 Comparison of predicted and experimental MR for Exp. I.

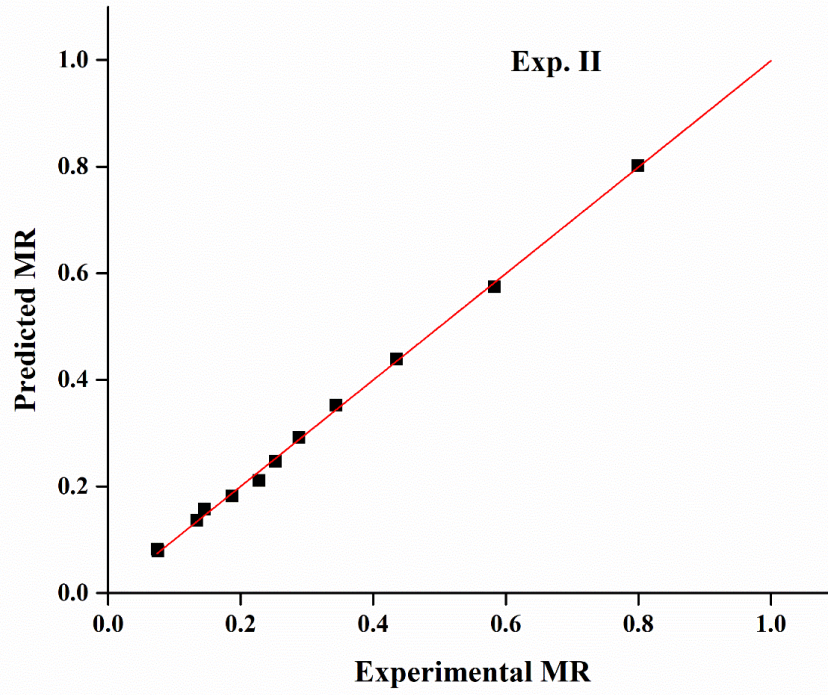


Figure 4.20 Comparison of predicted and experimental MR for Exp. II.

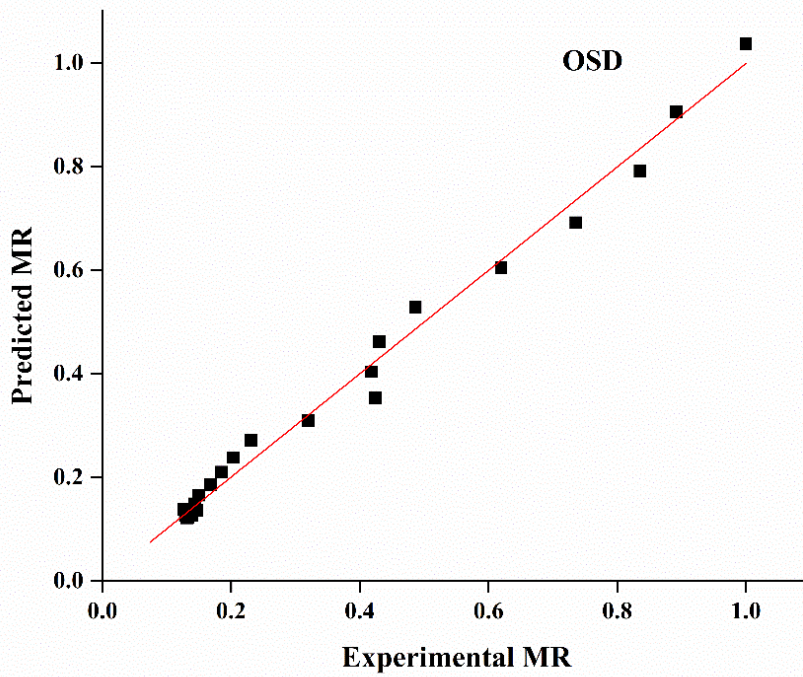


Figure 4.21 Comparison of predicted and experimental MR for OSD.

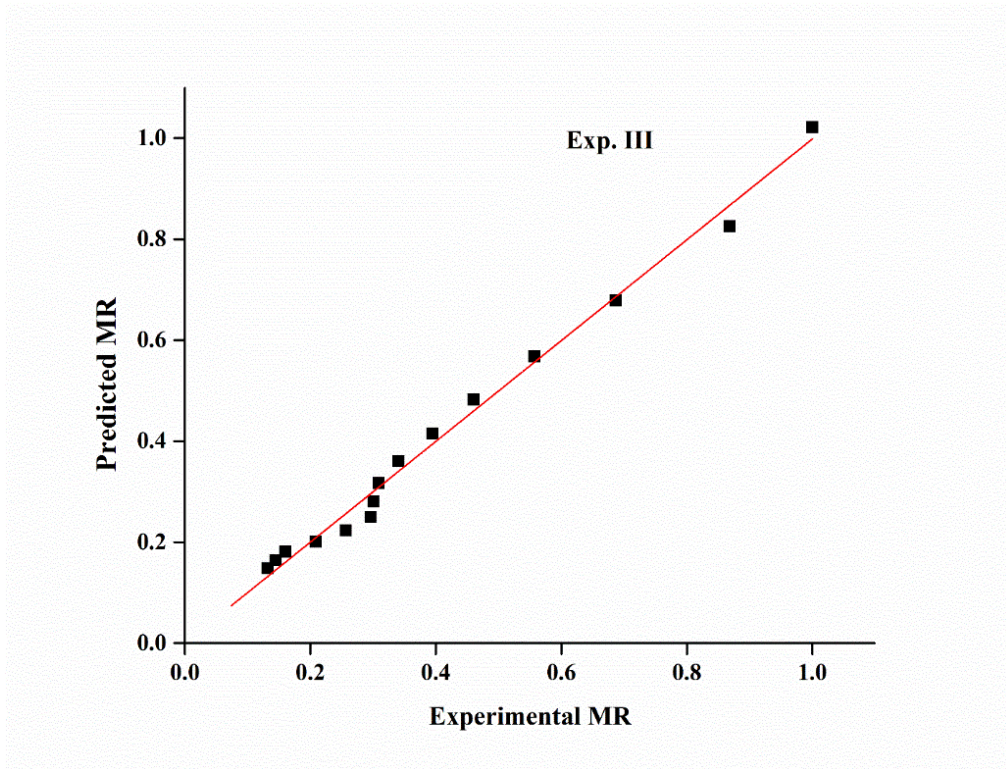


Figure 4.22 Comparison of predicted and experimental MR for Exp. III.

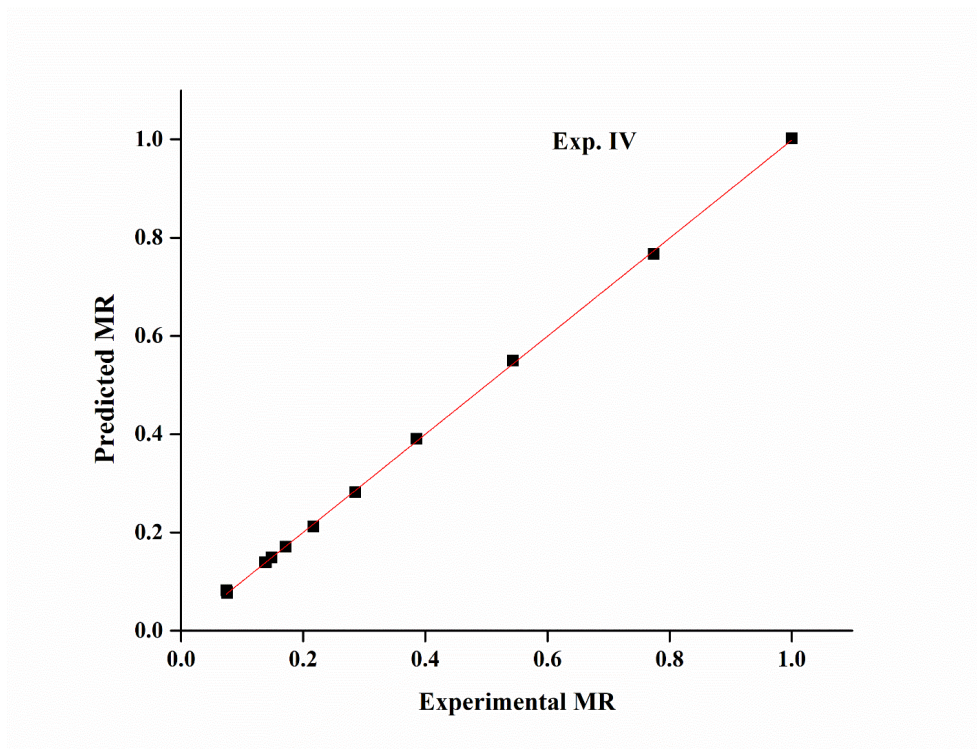


Figure 4.23 Comparison of predicted and experimental MR for Exp. IV.

Table 4.5 Fitting statistics of thin layer drying model of Exp. I of GP.

Model No.	Coefficients and constants	R^2	χ^2	$RMSE$
A.	$k = 0.1457$	0.9788	0.0015	0.03772
B.	$k = 0.1976; n = 0.8462$	0.9902	0.0007	0.02656
C.	$k = 0.2215; n = 0.6576$	0.9788	0.0015	0.03904
D.	$k = 0.1386; a = 0.9586$	0.9823	0.0012	0.03563
E.	$a = 0.7968; b = -0.3073; c = 0.5105;$ $g = 22.59; h = 1.123; k = 0.114$	0.9926	0.00053	0.02731
F.	$a = 0.8919; k = 0.09977; c = 0.1828$	0.9883	0.0008	0.03017
G.	$a = 0.7949; k_1 = 0.114; b = 0.4999;$ $k_2 = 1.092$	0.9929	0.00051	0.02449
H.	$a = 0.2271; k = 0.4966$	0.9917	0.00059	0.02444
I.	$a = -0.1267; b = 0.004832$	0.9654	0.0024	0.0499
J.	$a = 0.243; b = 0.2287; k = 0.4835$	0.9917	0.00059	0.02531
K.	$a = 1.014; b = -0.000272; k = 0.2078;$ $n = 0.825$	0.9904	0.0006	0.02836

Table 4.6 Fitting statistics of thin layer drying model of Exp. II of GP.

Model No.	Coefficients and constants	R^2	χ^2	$RMSE$
A.	$k = 0.2395$	0.9828	0.00153	0.03711
B.	$k = 0.3469; n = 0.7712$	0.9952	0.00042	0.02058
C.	$k = 0.6545; n = 0.366$	0.9827	0.00154	0.0393
D.	$k = 0.2336; a = 0.9785$	0.9829	0.00152	0.03901
E.	$a = -6.909; b = 0.3508; c = 7.577;$ $g = 0.0993; h = 0.3231; k = 0.3157$	0.9962	0.00034	0.02475
F.	$a = 0.9052; k = 0.319; c = 0.1067$	0.9954	0.00041	0.02156
G.	$a = 0.6604; k_1 = 0.715;$ $b = 0.5498; k_2 = 0.1395$	0.9973	0.00024	0.01764

H.	$a = 0.3296; k = 0.5303$	0.9941	0.00052	0.02299
I.	$a = -0.206; b = 0.01245$	0.9789	0.00188	0.04339
J.	$a = 0.8728; b = 0.0618; k = 0.3181$	0.996	0.00036	0.02012
K.	$a = 1.008; b = 0.009418;$ $k = 0.2796; n = 1.016$	0.9959	0.00036	0.02162

Table 4.7 Fitting statistics of thin layer drying model of OSD of GP.

Model No.	Coefficients and constants	R^2	χ^2	$RMSE$
A.	$k = 0.1256$	0.9822	0.000557	0.03749
B.	$k = 0.256; n = 0.4613$	0.9421	0.001817	0.07119
C.	$k = 0.3327; n = 0.3776$	0.9822	0.000557	0.03841
D.	$k = 0.1283; a = 1.02$	0.9828	0.000539	0.0378
E.	$a = -1.239; b = 0.9772; c = 1.259;$ $g = 0.1241; h = 1.034; k = 1.163$	0.9839	0.000505	0.04089
F.	$a = 0.9879; k = 0.1492; c = 0.05401$	0.9859	0.000442	0.03511
G.	$a = 0.0001123; k_1 = -0.3112;$ $b = 1.036; k_2 = 0.1351$	0.9889	0.000347	0.03198
H.	$a = 0.6064; k = 0.1541$	0.9827	0.000543	0.03793
I.	$a = -0.1044; b = 0.00308$	0.9888	0.000351	0.03051
J.	$a = 0.5052; b = 0.222; k = 0.3583$	0.9818	0.000518	0.03615
K.	$a = 0.9792; b = 0.9559; k = 1.147;$ $n = 0.9558$	0.9809	0.000599	0.04321

Table 4.8 Fitting statistics of thin layer drying model of Exp. III of GP.

Model No.	Coefficients and constants	R^2	χ^2	$RMSE$
A.	$k = 0.1623$	0.9748	0.00188	0.04182
B.	$k = 0.2193; n = 0.84$	0.9871	0.00096	0.03113

C.	$k = 0.4354; n = 0.3727$	0.9748	0.00188	0.0434
D.	$k = 0.1554; a = 0.9637$	0.9774	0.00169	0.04111
E.	$a = -12.03; b = 13.11; c = -0.1308;$ $g = 0.1777; h = 0.638; k = 0.1782$	0.965	0.00262	0.06156
F.	$a = 0.8876; k = 0.1214; c = 0.2224$	0.9891	0.00081	0.02969
G.	$a = 0.5392; k_1 = 0.09363;$ $b = 0.4829; k_2 = 0.3671$	0.9912	0.00066	0.02795
H.	$a = 0.2712; k = 0.4486$	0.9894	0.00079	0.02817
I.	$a = -0.1413; b = 0.005977$	0.962	0.00284	0.05336
J.	$a = 0.4875; b = 0.2732; k = 0.3338$	0.9906	0.00070	0.02769
K.	$a = 1.017; b = 0.004103;$ $k = 0.2193; n = 0.9017$	0.9887	0.00084	0.03156

Table 4.9 Fitting statistics of thin layer drying model of Exp. IV of GP.

Model No.	Coefficients and constants	R^2	χ^2	RMSE
A.	$k = 0.2913$	0.9888	0.00114	0.03186
B.	$k = 0.3182; n = 0.934$	0.9902	0.001	0.03168
C.	$k = 0.5986; n = 0.4865$	0.9888	0.00114	0.03379
D.	$k = 0.2906; a = 0.9978$	0.9888	0.00114	0.03378
E.	$a = 0.2663; b = -3.682; c = 4.41;$ $g = 0.242; h = 0.2448; k = 0.4043$	0.99	0.00102	0.04528
F.	$a = 0.9432; k = 0.3634; c = 0.07876$	0.9958	0.00042	0.02214
G.	$a = 0.00118; k_1 = -0.4715;$ $b = 1.015; k_2 = 0.316$	0.998	0.00020	0.01656
H.	$a = 0.4455; k = 0.4677$	0.9922	0.000791	0.02813
I.	$a = -0.2441; b = 0.0169$	0.993	0.00070	0.02664
J.	$a = 0.9993; b = -1.708; k = 0.3085$	0.9976	0.00024	0.01679
K.	$a = 1.002; b = 0.01305;$ $k = 0.2851; n = 1.185$	0.9998	0.00002	0.0052

A comparison of different performance parameters of all four and OSD experiments is shown in Table 4.10. The photos of fresh and dried GP from the experiments are shown in Figure 4.24, Figure 4.25, Figure 4.26, Figure 4.27, Figure 4.28, and Figure 4.29. It was observed that the color, taste, aroma, and texture of GP dried in Exp. IV were superior. This is due to the single day drying in Exp. IV. The extended drying period in Exp. I, Exp. II, Exp. III and OSD resulted in low-quality final product due to microbial growth.



Figure 4.24 Fresh GP



Figure 4.25 Dried GP in
Exp. I.



Figure 4.26 Dried GP in
Exp. II.



Figure 4.27 Dried GP in Exp.
III.



Figure 4.28 Dried GP in
Exp. IV.



Figure 4.29 Dried GP in
OSD.

Table 4.10 Performance parameters of the solar dryer for Exp. I, Exp. II, Exp. III and Exp.

IV

Parameter	Exp. I	Exp. II	Exp. III	Exp. IV	OSD
Maximum inlet temperature of the dryer (°C)	66.4	71.3	67.9	71.9	-
Drying time (h)	31 h	26 h	28 h	10 h	53
Average Dryer efficiency (%)	18.12	22.37	21.74	24.46	-
Lowest SEC (kWh/kg)	5.87	5.73	5.81	5.33	-
Initial MC (% w.b.)	87.99	87.99	87.99	87.99	87.99
Final MC (% w.b.)	12.09	12.09	12.09	12.09	12.09
Best Drying Model	Two-Term	Two-Term	Two-Term	Midilli and Kucuk	Two-Term

4.4.3 Economic analysis

The growth of the economy of the product depends on how it is processed. Currently, the solar dryer estimated cost were 25000 INR, 27000 INR, 26000 INR, and 28000 INR for Exp. I, Exp. II, Exp. III and Exp. IV, respectively. The price of gravel has been added for Exp. III and Exp. IV. The inflation rate has been set at 5.20 %, and the rate of interest has been set at 10 %. The expected lifespan of the dryer is 20 years. The life cycle savings have been calculated using the life cycle price keeping in mind the long-term economic benefits of the solar dryer. Additionally, the payback period, a key indicator of economic feasibility in any production system, has been established. Table 4.11 provides an estimate of the price of the solar dryer with and without storage. The savings for drying GP using solar energy have been calculated in comparison to branded goods that are readily available on the open market. When comparing the price of the solar-dried product with the price of commercially labelled GP, the price of additional post-harvest processes, such as washing and packing, has also been added. GP is sold for 900 INR per kg in the Indian market. Savings for the base year were determined to be 148 INR, 249 INR, 166 INR, and 426 INR per day for Exp. I, Exp. II, Exp. III and Exp. IV, respectively. The payback period of the developed dryer, estimated using was 1.6 years, 0.9 year, 1.4 years, and 0.59 year for Exp. I, Exp. II, Exp. III and Exp. IV, respectively. This was estimated for 120 days per year. This amount is considerably lower than the dryer's useful life (normally 20 years). This payback period only applies to drying one product. But different seasonal vegetables and fruits are nearly always

dried throughout the year. Consequently, the value of the payback period will decrease. As a result, the payback period for this dryer is quite low compared to its life (20 years).

Table 4.11 Economic study of Exp. I, Exp. II, Exp. III and Exp. IV for GP.

Items	Exp. I	Exp. II	Exp. III	Exp. IV
Price of the development of the dryer in INR	25000	27000	26000	28000
Predicted lifespan of the dryer	20 years	20 years	20 years	20 years
Price of fresh GP in INR	70 per kg	70 per kg	70 per kg	70 per kg
Interest rate	10 %	10 %	10 %	10 %
Inflation rate	5.20 %	5.2 %	5.20 %	5.2 %
Annualized capital price in INR	2936	3171	3054	3289
Maintenance price in INR	294	317	305	329
Salvage value in INR	2500	2700	2600	2800
Annual salvage value in INR	44	47	45	49
Annualized price in INR	3186	3441	3314	3569
Price of dried GP available in market in INR	900 per kg	900 per kg	900 per kg	900 per kg
Savings in INR	148	249	166	426
First-year annual savings in INR	17810	29900	19932	51151
Payback period (1 US\$=74.57 INR)	1.6 years	0.9 year	1.4 years	0.59 year

4.5 Summary

The development of a novel active solar dryer capable of operating in the indirect and mixed modes, their performance studies on the drying of GP, the drying kinetics, and economic analysis of GP is presented. For the studies, the work was divided into four sets of experiments with OSD: indirect solar drying without SHS (Exp. I), mixed-mode solar drying without SHS (Exp. II), an indirect solar drying with SHS (Exp. III), and mixed-mode

solar drying with SHS (Exp. IV). The following conclusions were inferred from the experiments:

- During 17:00-18:00 h, the output temperature of SAC with SHS was (2.5-6.7) °C higher than the ambient temperature (Exp. IV). This is because the heat was stored in these SHS materials throughout the day and released when the solar radiation is insufficient.
- The maximum efficiencies of SAC without the SHS were 72.86 %, 72.97 %, 73.34 %, and 71.79 %, respectively on Day 1, Day 2, Day 3, and Day 4, whereas with SHS were 83.56 %, 85.29 %, and 85.52 %, respectively on Day 5, Day 6 and Day 7.
- The average efficiencies of the dryer for Exp. I, Exp. II, Exp. III and Exp. IV were calculated as 18.12 %, 22.37 %, 21.74 % and 24.46 %, respectively. If all the four experiments were taken into consideration, it could be observed that, Exp. I had the least efficiency and Exp. IV had the most. This is due to the high moisture removal rate in a mixed-mode solar dryer and the addition of SHS material inside the SAC in Exp. IV. The lowest SEC for Exp. I, Exp. II, Exp. III and Exp. IV were calculated as 5.87, 5.73, 5.81 and 5.33 kWh/kg, respectively.
- In all four sets of experiments along with OSD, the MC of GP was reduced to 12.09 % (w.b.) from 87.99 % (w.b.). For Exp. I, Exp. II, OSD, Exp. III, and Exp. IV, the overall drying times were 31, 26, 53, 28, and 10 h, respectively. Eleven models were evaluated to select suitable drying models; the Two-Term model was the best-fitted model for Exp. I, Exp. II, OSD, and Exp. III. For Exp. IV, the Midilli and Kucuk model was found to be the best fit.
- The lower values of SEC and higher values of SAC efficiency and dryer efficiency clearly demonstrated higher performance in mixed mode solar dryer with sensible heat storage (Exp. IV).
- The construction of the dryer for Exp. I, Exp. II, Exp. III and Exp. IV was around 25,000, 27,000, 26,000, and 28,000 INR, respectively for 120 usage days in a year. The payback period, a direct economic measure, is particularly attractive. The calculated economic payback periods for Exp. I, Exp. II, Exp. III and Exp. IV, respectively, are 1.6 years, 0.9 years, 1.4 years, and 0.59 years.